

Validation of a Three-Dimensional Transmission Line Matrix (TLM) Model Implementation of a Mode-Stirred Reverberation Chamber

Alyse Coates, *Member, IEEE*, Hugh G. Sasse, Dawn E. Coleby, Alistair P. Duffy, *Senior Member, IEEE*, and Antonio Orlandi, *Fellow, IEEE*

Abstract—Reverberation chambers are attractive electromagnetic compatibility test facilities, both economically and technically. Careful design and analysis of these facilities are important, if the results obtained are to be treated with a high level of confidence. Numerical modeling is an important part of the process of reverberation chamber design and analysis. Hence, it is important that the modeling techniques to be used are appropriately validated. Much of the published work to date takes either a statistical or a deterministic view of validation. This paper provides validation evidence for a low-resolution transmission line matrix (TLM) model of a reverberation chamber in a manner approximating the way in which the chamber is used, i.e., validating based on the effects of a simple device under test. A variety of statistical and heuristic approaches have been used to quantify the level of agreement, intending to set the likely lower bound for the quality of comparisons between simulations and measurements. While not drawing any “universal” conclusions about the veracity of the TLM technique, the paper concludes that a relatively simple model of a reverberation chamber provides a useful analysis of the chamber with close comparisons between modeled and measured data.

Index Terms—Mode-stirred chamber, reverberation chamber, test facilities, transmission line matrix (TLM), validation.

I. INTRODUCTION

REVERBERATION chambers are increasingly popular as electromagnetic compatibility (EMC) test sites because of their ability to provide a statistically uniform field within a relatively large volume, to generate high-peak fields from comparatively modest input powers, to isolate the test environment from a potentially noisy ambient environment, and to provide a lower cost alternative to anechoic chambers or open-area test sites. Clearly, these benefits can deliver both technical and economic advantages to industry and academia. However, the operational benefits of the chambers can only be maximized when their behavior is well understood. This understanding can be obtained through experimentation, and through mathematical analysis and modeling. This paper is concerned primarily

with the validation of modeling results against experimental data. Validation can be undertaken at the level of validating the general performance of a technique, the implementation of this technique into a package or the manner in which this implementation has been used to model specific systems [1]. This paper is primarily interested in the quality of comparison between a relatively low-resolution transmission line matrix (TLM) model and measurements. Models are intended to reflect only the aspects of a system of interest in order to permit decisions to be made effectively about systems that would be overcomplicated, or which would have unrealistic time and memory implications, if represented in “perfect” detail. The output from these simulations permits the construction of cognitive models, which, in themselves, facilitate reasoning about more complicated systems. Hence, the objective of validating these models is to determine when a model is good enough and not when it is “perfect,” effectively “satisficing” [2] rather than maximizing agreement.

A. Modeling and Validation

One validates a modeling technique or implementation so that it can be used to investigate questions that either cannot be answered directly by measurement, or which would be expensive to answer by experimentation. Some important problems for reverberation chambers are to determine the lowest useable frequency (LUF), or the converse of determining the specific dimensions of a chamber for a specific application [3]; to gain a better appreciation of the significance of results for emerging applications, such as antenna tests [4], or to test rules-of-thumb used in experimental design [5].

One of the most widely referenced papers on the use of modeling for the optimization of reverberation chambers is [6], which used finite-difference time domain (FDTD) in 2-D to show that a large mechanical stirrer produces a better result. A further study with FDTD that aims to decouple models from chamber Q -factors is [7]. Here, modeled results and measurements were compared directly when the Q -factor losses were added in as a post processing stage. These results showed a fair level of agreement with very good amplitude agreement, but notable differences in the individual features.

A further application of FDTD was used to show a good agreement with published results for frequency stirring [8].

Other techniques that have been used to model reverberation chambers include the boundary element method (BEM), whose

Manuscript received June 14, 2006; revised September 27, 2006 and February 20, 2007. This work was supported in part by Brand-Rex Ltd., Glenrothes, U.K.

A. Coates is with Lockheed Martin UK INSYS Ltd., Ampthill, Bedfordshire, MK45 2HD, U.K. (e-mail: alyse.coates@ieee.org).

H. G. Sasse and A. P. Duffy are with the Applied Electromagnetics Group, De Montfort University, Leicester LE1 9BH, U.K. (e-mail: hgs@dmu.ac.uk; apd@dmu.ac.uk).

D. E. Coleby is with the Department of Health Sciences, University of Leicester, Leicester LE1 6TP, U.K. (e-mail: dc55@leicester.ac.uk).

A. Orlandi is with the UAq EMC Laboratory, University of L'Aquila, L'Aquila I-67040, Italy (e-mail: Orlandi@ing.univaq.it).

Digital Object Identifier 10.1109/TEMC.2007.903697

relative advantages and disadvantages are discussed in [5], where statistical parameters are extracted and compared with measurements, showing good agreement, and TLM where [9] compares a number of models with measurements.

This is not an exhaustive list of modeling references, nor it is intended to be. A broader review of recent work can be found in [10], which provides a thorough review of the reasons for performing simulations. What has been illustrated is that there is a growing body of work in this field.

However, with this growing body of modeling results comes some further questions about how to actually perform the comparisons required for validation. For example, [10] suggests that the use of statistics to validate models may mask the real performance of the chamber because the authors claim that it is relatively easy to get statistically excellent agreement even if there is total disagreement between field simulations and measurements. It is suggested that this leads to the need to perform direct comparisons against measured near fields “without further data processing or statistical analysis.” However, it does not take into account the reasons for validating; if the aim is to use the reverberation chamber to give a known statistical distribution, then a statistical analysis is required. The implication of this is the need to be careful about what is being validated and why.

Another issue about the veracity of statistical analyses comes in [4], where the authors look to determine the effective number of independent samples from a given number of observations under the assumption that the average power is normally distributed. However, the assumption of Gaussian distribution may not be correct, which will lead to the determination of the error levels not being correct.

One of the most important observations in support of a statistical approach is in [3], which notes that because the received signals are dependent on neither the antenna orientation, nor on the antenna gain, it is logical to consider the operation of the chamber statistically with the fields having a Rayleigh or Rice distribution. In fact, [3] does suggest that the real answer to understanding reverberation chambers is not an either/or decision with statistical representations and direct results but a combination of both.

Another important aspect of the validation process, in addition to the balance between direct and statistical comparison, is what to measure. It is common to take field measurements at a point, or a number of points. However, [3] notes that care must be taken when looking at fields at points (particularly at the corners and the center of a working volume) because they may not be representative of where an EUT is placed. This provides a good reason for looking at all of the space in the chamber and for introducing a test object as well. Some support for this view can be seen in [11], where some difficulties were noted in the modeling of a loaded chamber, suggesting that the modeling of a loaded chamber is an important step in the validation of reverberation chambers. More recent investigation into the behavior of loaded chambers [12] raises a number of questions about the effects of loading, including the relationship between the metrics developed and the standard deviation of the fields. Investigation of these issues is well suited to a modeling approach, providing there has been some validation of the model. Additionally, [13]

notes the disruptive effect that measuring devices can have on local fields.

Clearly, there is a debate about the relative benefits of using a statistical versus a direct approach for validation, how much detail is required, and whether there is a better (or best) modeling technique.

The underlying assumption of this paper is that it is important to validate using approaches close to the manner of taking measurements in practice, including the introduction of a test object. In order to quantify the comparisons, a number of techniques are presented and compared. These are:

- 1) augmented visual approaches using scatter plots and box plots (Augmented indicates that this is in addition to the data as presented with respect to frequency);
- 2) statistical metrics based on correlation, parametric and nonparametric tests;
- 3) heuristics techniques, particularly feature selective validation (FSV).

These approaches will be reviewed and applied in Section IV.

B. Test Chamber

The chamber used for this validation exercise was 5 m × 2.95 m × 2.36 m (x -, y -, z -axis) giving a lowest useable frequency of approximately 180 MHz [14]. The stirrer design consisted of two 1 m square vanes set at 45°. The height of the vanes was alterable, and the stirrer was set as close to the corner of the chamber as possible, thus maximizing the “uncluttered” volume, containing the working volume. Using the approach discussed in [11], the stirrer can only be regarded as electrically large above approximately 300 MHz. There are, therefore, some regions of particular interest during validation:

- 1) $f < 180$ MHz (below lowest usable frequency);
- 2) $180 \text{ MHz} < f < 300$ MHz (electrically small stirrer);
- 3) $f > 300$ MHz (electrically large stirrer).

Measurements and simulations were performed between 50 and 500 MHz. The lower frequency being well below the minimum usable frequency and the upper value was, thus, above the transition to an electrically large stirrer.

The simulations were undertaken using a commercial TLM solver with the chamber described by a parallelepiped of the aforementioned dimensions with the stirrer shaft permanently located. The TLM method [15] was chosen over methods such as FDTD for this study because it is a technique that the authors have used successfully for previous reverberation chamber simulations (e.g., [9]) and investigating how simple an acceptable model could be is an important extension of this work. The vanes were included separately so that they could be rotated between simulations. Fig. 1 illustrates the practical setup and Fig. 2 shows the plan view.

This chamber was used to produce field strength measurements at the center of the “uncluttered” volume (the “output point” of Fig. 2) and electric field throughout the chamber at specific frequencies (100, 200, 300, 400, and 500 MHz). In these cases, no further objects were introduced into the model. Further, it was used to model the currents at specific positions along a wire.

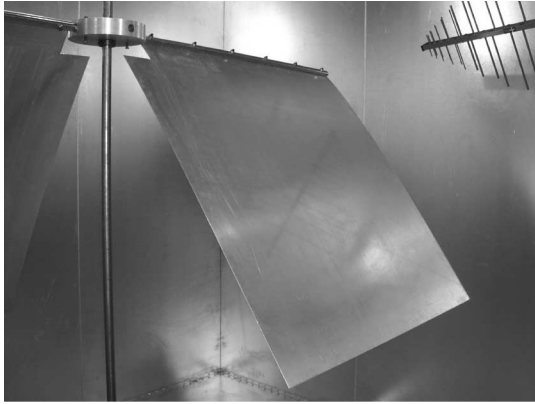


Fig. 1. Illustration of stirrer design.

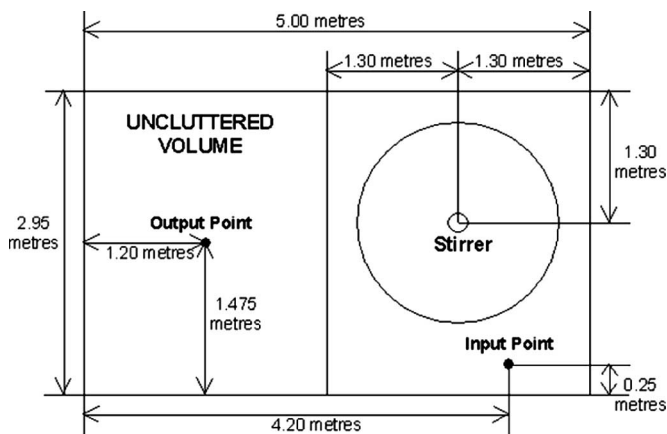


Fig. 2. Plan view of chamber showing layout.

The maximum cell size was 6 cm, giving a maximum frequency of 500 MHz (using the rule-of-thumb of allowing ten nodes per minimum wavelength). Metallic elements were included in the model using finite conductivities (approximately $7 \times 10^{-7} \text{ S}\cdot\text{m}^{-1}$). Where wires were introduced and at the location of the stirrer, the node size was reduced to 1 cm, these reductions applied along the plane, giving a maximum nodal aspect ratio of 6:1. Each of the stirrer positions was modeled separately, i.e., the results presented later in this paper are an amalgam of the separate simulations. Hence, in order to allow the suite of simulations to be run in an acceptable time, arbitrarily chosen as approximately one working day on the available computer (a 1.7-GHz Pentium IV with 512 MB of RAM), a run length of 8000 iterations was chosen (each simulation requiring 20 min). It should be noted that these choices have the potential to introduce noticeable errors because of the following factors.

- 1) The resolution of the stirrer has a high level of granularity, particularly when it is considered that the vanes are not parallel with any of the axes for most of the time, giving a marked step-like model compared to a smooth real stirrer. Any further reduction in the node size to improve the resolution would be accompanied by an increase in run time, and because the models are required to test the effects of a number of parameter changes, any decision to increase the run time is potentially expensive.

- 2) The choice of 8000 iterations will only allow the fields to partially decay, resulting in some imprecision of the results. However, in order to allow the fields to decay to a vanishingly small amount allowing a more accurate frequency response, each simulation would have to run for 600 000 steps, which would have a huge impact on the run time.
- 3) Both measurements and simulations used 20 stirrer steps over half a revolution: the stirrer is rotationally symmetrical. A more practical implementation would use more stirrer steps, typically 200, which would increase the run time but reduce the potential for locational errors.
- 4) In the actual measurements, a bilog antenna was used, but a line impulse excitation was used in the models to reduce the burden on the simulations.

Hence, with these limitations, it is important to identify whether the models are “fit for purpose,” particularly considering that if all the (200) stirrer positions were modeled with a run time close to ideal, even without an increase in spatial resolution, the total run time requirement would be approximately 200 days! It should be noted that this simulation was impulse excited, allowing the question “after how many iterations is the frequency response good enough?” to be asked. A total of 8000 iterations was a value that showed the resonances starting to form and appear as distinct entities. Accurate and precise modeling (such as [16]) would require several hundred thousand iterations to allow the fields to decay (if impulse excited) or to achieve stability, if continuous wave (CW) excited (as in [16]). However, it is worth restating that the purpose of this paper is to determine whether a set of known assumptions can be applied to the modeling, and still provide results that are “good enough,” as, perhaps, a precursor to a more accurate, but substantially more time-consuming full study.

C. Overview of Paper

This paper is interested in the validation of TLM modeling of a reverberation chamber against experimental results. This introductory section has reviewed some of the current body of knowledge, and in doing so, has noted that there is no generally accepted means of undertaking the validation with some authors favoring purely statistical means and others direct comparison.

The next section looks at field measurement validation using the stirring ratio both at a point and throughout the chamber volume. This is followed by the comparison of measured and modeled currents on a test object and a section on the quantitative analysis of the results, where representative results from the two sections are compared with visual assessment using statistical and heuristic techniques. The paper finishes with a discussion and conclusion, including an overview of the significance of this research.

II. STIRRING RATIO

The purpose of mode stirring is to move the field profile—the peaks and nulls—around the chamber. A simple method for measuring this is the stirring ratio. The stirring ratio is the ratio of the minimum (E_{MIN}) to maximum (E_{MAX}) electric field

TABLE I
COMPARING THE STIRRING RATIOS PRODUCED IN
THE REAL AND SIMULATED CHAMBERS

Vane Height (metres)	Mean of stirring ratio between 200MHz and 500MHz (dB)		Difference between means (dB)
	Simulated chamber	Real chamber	
0.88	10.84	11.27	-0.43
1.08	11.23	11.24	-0.01
1.28	11.83	11.37	0.46
1.48	12.02	11.39	0.63
1.68	12.18	11.55	0.63
1.88	12.09	11.23	0.86
2.08	11.92	11.26	0.66

strength measured at a defined point within the chamber over one revolution of the stirrer. Hence, the stirring ratio (*SR*) is

$$SR \text{ (dB)} = -20 \log_{10} \frac{E_{\text{MIN}}}{E_{\text{MAX}}} \quad (1)$$

While this measure is becoming less popular in formal tests, it still proves useful in quantifying the ability of the chamber to stir the modes as a function of frequency. It also provides some insight into the potentially worst case agreement between models and measurements because of the need to take ratios. As such, it is representative of many tests carried out in the reverberation chamber that require ratios to be taken, such as shielding effectiveness measurements.

As the stirrer rotates, the ability to locate a mode and null at a particular location is reflected in the stirring ratio. A stirring ratio that is uniformly high throughout the volume is indicative of efficient stirring in the chamber.

For each of the stirrer steps, the electric field was measured at an output point precisely in the center of the uncluttered volume, as indicated in Fig. 2. The electric field was similarly measured in the real chamber at the output point for each stirrer step.

To be able to compare simulations and experiments for one optimization task, the vane height was varied, and the results calculated for each (the stirrer height being calculated from the floor of the chamber to the top of the vane). The stirrer height varied between 0.88 and 2.08 m in 0.2 m increments and the stirring ratio calculated for both measurements and simulations, thus requiring seven sets of simulations, which required a few days of simulations compared to the several years that would have been required if the simplifications in Section I-B had not been implemented. To observe the general trend in these results, the mean stirring ratio responses between 200 and 500 MHz were calculated and compared in Table I, thus ignoring the frequency range below the minimum working frequency.

Table I shows that there is demonstrable consistency between the results, suggesting that the simulated chamber is an acceptable representation of the actual chamber.

To test the assertion of whether the central output point was representative of the results for the entire chamber, the stirring ratio was calculated for every point within the chamber across all the chamber's frequency regions at five different frequencies (100, 200, 300, 400, and 500 MHz) and for each of the seven vane heights. The implication of the lack of representativeness is that a larger number of comparisons would be required to

TABLE II
SHOWING HOW THE MEAN OF THE STIRRING RATIO (DECIBELS) IN THE ENTIRE CHAMBER CHANGES WITH VANE HEIGHT AND FREQUENCY

Vane Height (m)	100MHz	200MHz	300MHz	400MHz	500MHz
0.88	17.16	15.93	11.84	11.84	11.14
1.08	17.94	14.75	11.46	12.05	11.62
1.28	17.52	15.05	12.16	12.15	12.00
1.48	17.23	14.25	12.84	12.57	11.86
1.68	17.82	13.99	13.31	12.78	11.79
1.88	19.33	14.32	12.52	12.48	11.49
2.08	20.21	13.76	11.92	11.81	11.27

TABLE III
SHOWING HOW THE STIRRING RATIO AT THE CENTER POINT CHANGES WITH VANE HEIGHT

Vane Height (m)	100MHz	200MHz	300MHz	400MHz	500MHz
0.88	16.94	12.82	10.61	9.975	10.86
1.08	16.82	14.31	10.69	9.734	10.60
1.28	17.64	13.75	12.24	10.44	10.62
1.48	17.42	13.30	11.10	11.01	10.98
1.68	18.34	12.92	12.45	10.35	11.44
1.88	19.22	13.41	12.74	10.75	10.91
2.08	17.80	14.18	11.37	11.19	10.81

TABLE IV
SHOWING THE DIFFERENCES BETWEEN THE STIRRING RATIOS OVER THE ENTIRE CHAMBER AND AT THE CENTER POINT

Vane Height (m)	100MHz	200MHz	300MHz	400MHz	500MHz
0.88	0.22	3.11	1.23	1.87	0.28
1.08	1.12	0.44	0.77	2.32	1.02
1.28	-0.12	1.30	-0.88	1.71	1.38
1.48	-0.19	0.95	1.74	1.56	0.88
1.68	-0.52	1.07	0.86	2.43	0.35
1.88	0.11	0.91	-0.22	1.73	0.58
2.08	2.41	-0.42	0.55	0.62	0.46

demonstrate validation of the model. The mean stirring ratio across the entire chamber was then calculated. The results are displayed in Table II, and the results for the central output point are displayed in Table III.

As can be seen by comparing Tables II and III, the stirring ratio at the central output point appears to be a representative of the mean stirring ratio for the entire chamber. The difference between the two was calculated, and is shown in Table IV.

The results shown in Table IV indicate that the stirring ratio results obtained from the central output point are, indeed, acceptably close to the mean stirring ratio in the entire chamber. Also, this central point can be used to calculate the stirrer efficiency over the entire frequency range and not just at specific frequencies. Therefore, this point can be used to gauge the effect of variations, such as the stirrer height, on the stirring ratio within the chamber, and hence, the likely impact on measurements. The upshot of this is that the comparison at the central point should be sufficient to provide a reasonable level of confidence in the overall quality of comparison between models and measurements. This is illustrated in Figs. 3 and 4 for

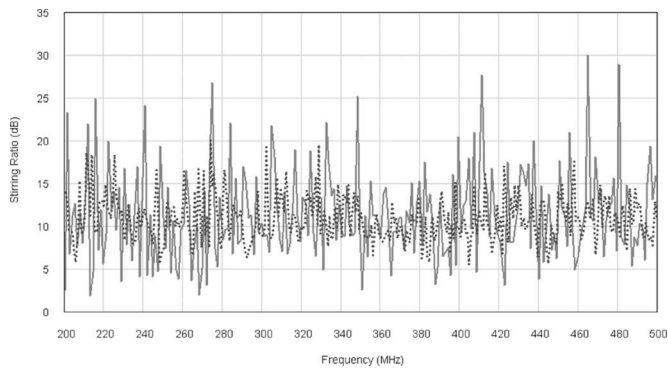


Fig. 3. Comparing the chamber and simulation results for a vane height of 0.88 m. The solid line is the measured results, and the dashed line is the simulated results.

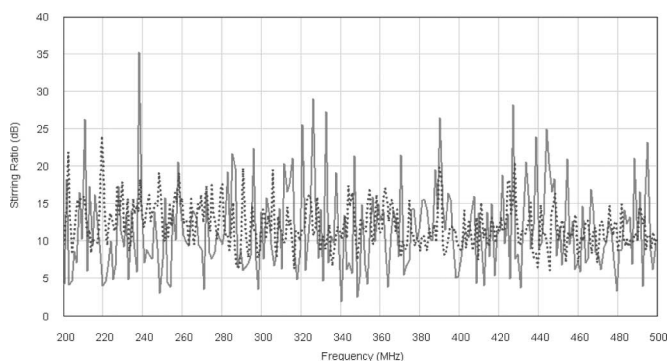


Fig. 4. Comparing the chamber and simulation results for a vane height of 1.48 m. The solid line is the measured results, and the dashed line is the simulated results.

stirrer heights of 0.88 and 1.48 m, which shows the stirring ratio results above the minimum working frequency. As can be seen, there is an encouraging level of correlation between the real and simulated chamber results.

It should also be noted that while the general resolution of these diagrams is quite low (due to the column width limitations), they are presented in the manner that they would normally be viewed, with a more detailed subdomain analysis following, if required, in the investigation of specific anomalies.

This section has provided some indication that there is a reasonable level of agreement between models and measurements in the three frequency zones mentioned earlier using field-based measurements. The next section looks at the effects of adding a test object into the chamber.

III. ADDING A TEST OBJECT

In order to compare the simulated and measured performance of the chamber with a test object in place, a wire was added to the simulation to represent a cable under test. This cable was 1-m-long wire with output points (at which the currents were measured) at 0.1-m intervals. This test cable was placed such that its center was in the center of the “uncluttered volume” and its axis was aligned with the x -axis of the chamber. This configuration is shown in Fig. 5.

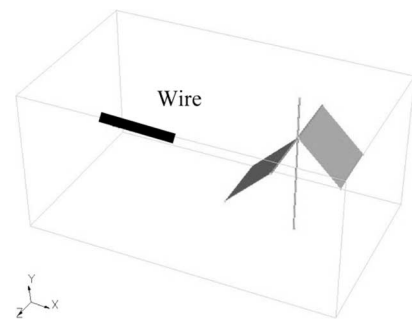


Fig. 5. Showing the orientation and location of the wire simulated in the chamber.

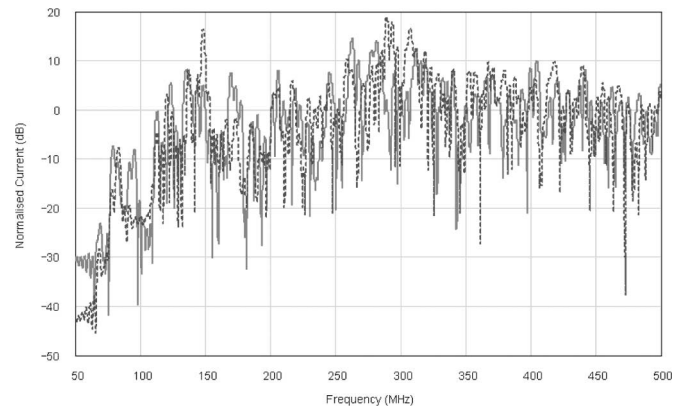


Fig. 6. How the simulated current at point 7 on the wire oriented in the x -direction varies with frequency and stirrer position. Solid line is stirrer position 0, and dashed line is stirrer position 9.

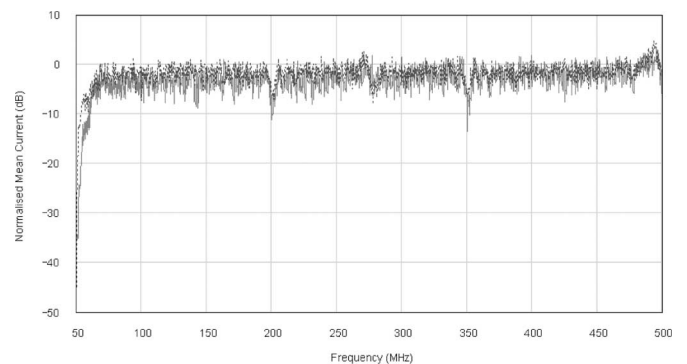


Fig. 7. Comparing the mean current obtained at point 1 for the real and simulated wires. Solid line is simulated, and dashed line is measured.

The currents on the cable were simulated over one stirrer revolution and measured for the frequency range 50–500 MHz, spanning the three zones discussed earlier.

Fig. 6 verifies the effect of the stirrer on the current at any point along the cable: this figure shows point 7 (i.e., midway between the center and the end nearest to the stirrer).

A comparison of modeled and simulated results is presented in Figs. 7 and 8, which show the normalized mean current at point 1 (end of the wire) and point 5 (center), respectively.

These figures show reasonably close agreement between the measured and simulated results over the entire frequency range. It is particularly reassuring to note the agreement of the features

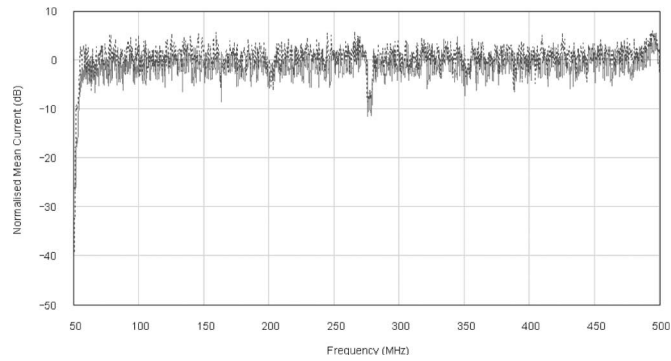


Fig. 8. Comparing the mean current obtained at point 5 for the real and simulated wires. Solid line is measured, and dashed line is simulated.

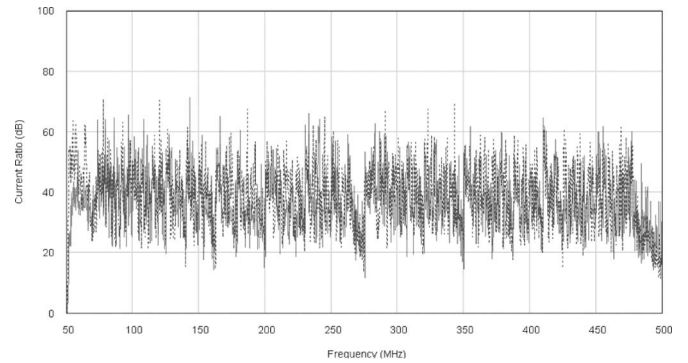


Fig. 10. Comparing the current ratios obtained from the real and simulated results at point 5. Solid line is measured, and dashed line is simulated.

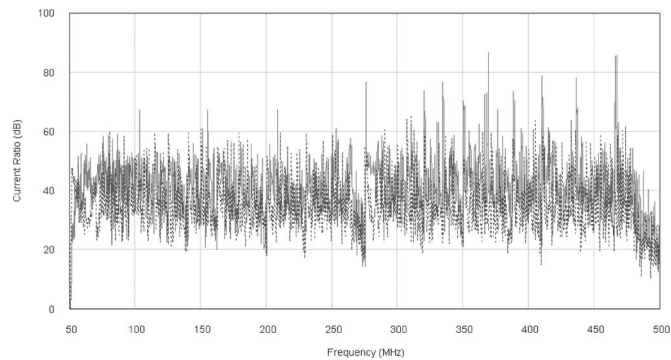


Fig. 9. Comparing the current ratios obtained from the real and simulated results at point 1. Solid line is measured, and dashed line is simulated.

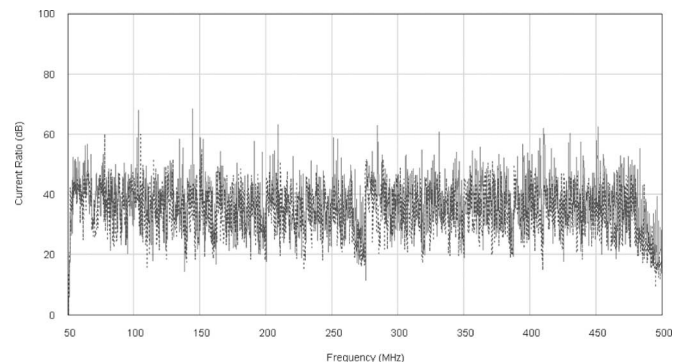


Fig. 11. Comparing the current ratios obtained from the real and simulated results at point 7. Solid line is measured, and dashed line is simulated.

in Fig. 7 at frequencies of 200 and 350 MHz, and in Fig. 8, at 280 MHz. However, just considering the mean current at a point does not provide a complete representation of the results, as the maximum and minimum currents, and hence, the maximum and minimum field strengths to which the wire is subjected, need to be taken into account. This amplifies the spread of values, giving some measure of the likely worst case agreement between models and measurements. To examine more closely the effect of the maxima and minima, a “current ratio” (IR) was obtained for each point over the frequency range. The current ratio was defined as the ratio of minimum (I_{MIN}) to maximum (I_{MAX}) current for each point, as obtained over one rotation of the stirrer, for all frequencies in the range [as noted in (2)]

$$IR \text{ (dB)} = -20 \log_{10} \frac{I_{MIN}}{I_{MAX}}. \quad (2)$$

The simulated and measured current ratio for three points 1, 5, and 7 are compared in Figs. 9–11. In each case, the current ratios appear to agree within 5 dB of each other, as indicated in Fig. 12 that compares the means of both measured and simulated current ratios, indicating a reasonable degree of similarity between the actual and simulated results.

Having presented results that appear to (visually) validate the model against measurements, it is important that additional objective approaches are used to quantify the agreement between these results. The next section addresses this.

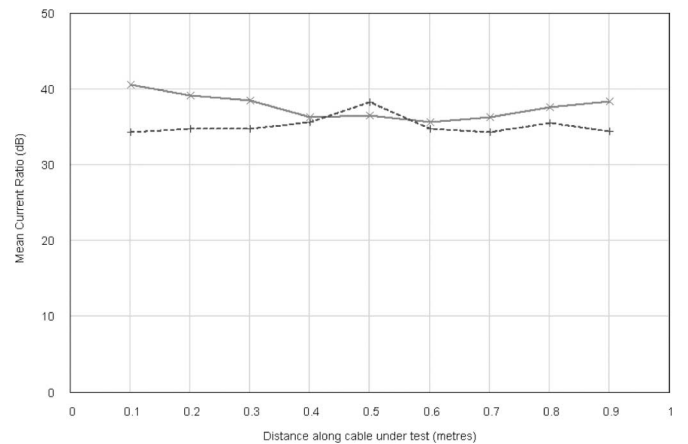


Fig. 12. Comparing the mean current ratios obtained from the real and simulated chambers. Solid line is simulated, and dashed line is measured.

IV. QUANTITATIVE ANALYSIS

It was noted in the Section I that care needs to be exercised regarding what is being validated and why. Clearly, where the need is for a field distribution to adequately represent a terrestrial propagation environment over a given frequency range, a comparison with a Rayleigh or Rice distribution is required. On the other hand, if there is a need to assess the performance of a device under test, for example, looking for poor shielding effectiveness, then there is a need to compare specific features

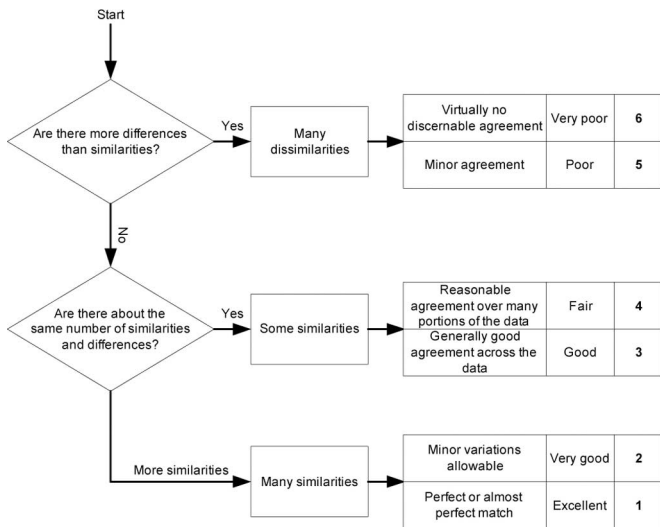


Fig. 13. Visual rating scale (adapted from [17]).

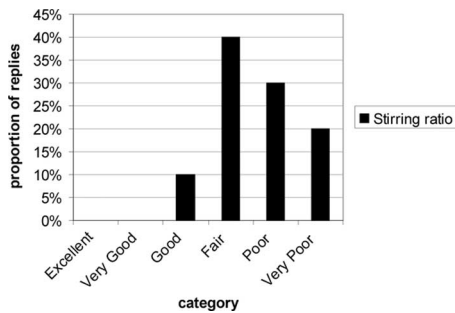


Fig. 14. Visual assessment of the data of Fig. 4.

as functions of frequency. The quantification of these requires different approaches. Many of the statistical tests were developed to compare the probability distributions (whether based on the mean in the case of parametric tests or on the shape of the probability distributions in the case of nonparametric tests). This gives us the opportunity to consider using, for example, the *t*-test, analysis of variables (ANOVA), or the Kolmogorov–Smirnov (KS) test. The choice is more limited when it comes to comparing the “shapes” of the original data, resulting in the use, primarily, of heuristic approaches such as the feature selective validation (FSV) method. This section will provide a brief overview of some of the most appealing techniques and will apply them to representative data from the previous sections (the field data of Fig. 4 and the current data of Fig. 10).

The presentation of data in the paper so far has relied on visual interpretation for assessment. Most engineers involved in undertaking models or measurements with systems such as the reverberation chamber will use that experience in assessing the quality of the comparisons [17].

In order to provide some baseline for the quantified assessment of the tests, visual assessment of two of the results (Figs. 4 and 10) was provided by ten reverberation chamber experts using the rating chart [17] of Fig. 13.

The results of these comparisons are given in Figs. 14 and 15.

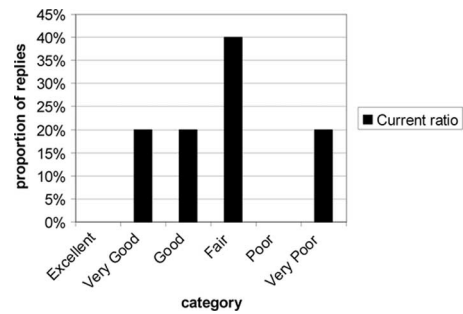


Fig. 15. Visual assessment of the data of Fig. 10.

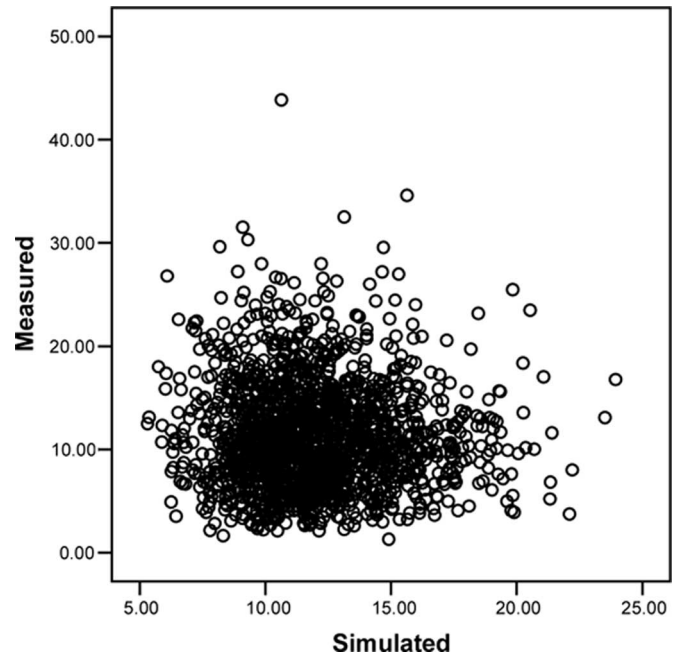


Fig. 16. Scatter plot for the stirring ratio data in Fig. 4. All units in decibels.

Even within statistics, visual interpretation of data comparisons is regarded as an important part of the analysis [18], and two tools to assist this visual interpretation are scatter plots and box plots [18]–[20] that are also useful in helping to interpret correlation, which is, perhaps the simplest approach to statistical analysis of data. The most common correlation technique is the Pearson *r* correlation. However, correlation can break down if there are many outliers (data points outside what appears to be the normal range). Such outliers are part-and-parcel of the electromagnetic systems such as reverberation chambers, where they arise from occasional very high or very low values. To ignore them may be a justifiable way to improve the level of agreement, but equally ignoring the outliers may result in valid data being rejected. *Scatter plots* present the values of one data set against the values from the other. The slope of the resulting regression line is the Pearson *r* value.

Figs. 16 and 17 show the scatter plots for the data of Figs. 4 and 10. The correlation coefficient for Fig. 16 is -0.38 , and for Fig. 17, it is 0.401 . Each circle represents the measured versus modeled results at a (paired) frequency point. The stronger the association between the two data sets, the closer the circles align

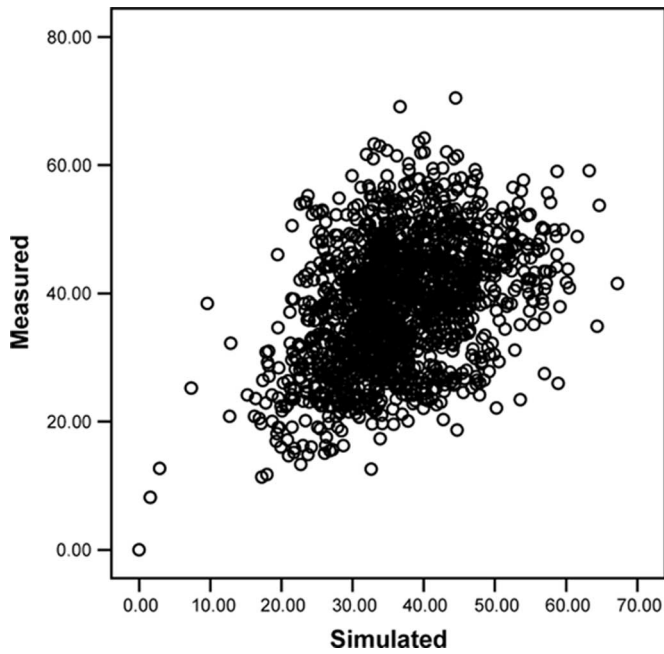


Fig. 17. Scatter plot for the current ratio data in Fig. 10. All units in decibels.

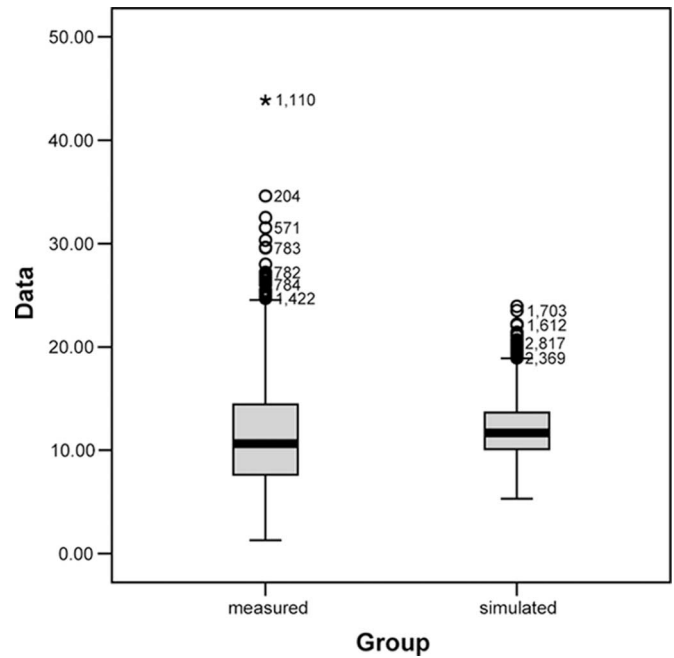


Fig. 18. Box plot of the stirring ration data of Fig. 4.

along the leading diagonal, giving a correlation coefficient of +1 (or on the trailing diagonal for $r = -1$) These figures show that the relationship between the two sets of data is very weak, and in the case of the stirring ratio results, almost nonexistent, which does not entirely agree with the visual interpretation of the original data; however, it does show that there is a wide variation in the point-by-point agreement of the data, which is visually supported by noting the “grassiness” of the original data. More information can be garnered from box plots that provide a summary view of the distribution of the data by displaying the median value as a line in a box that usually represents the lower and upper quartiles. Fences are then added to the extremes of the boxes to show the deciles.

Figs. 18 and 19 show the box plot comparisons. Outliers are represented by circles or stars (the numbers refer to the data set point number, which is useful when investigating the data).

These results suggest that there is a greater general agreement between the pairs of results, but both have a number of outliers that may have a bearing on the overall results. It is clear from these results that the median values and the interquartile ranges are reasonably close, but this is not sufficient to provide enough information on the probability distributions of the data.

It is not reasonable to assume that the probability distributions of the data are normal. Papers, such as [3], show that a Rayleigh or Rice distribution is closer. However, the central limit theorem [21], which suggests that parametric tests can be applied to nonnormal distributions provided that the sample size is large, allows the t -test (which evaluates the difference in means for two groups) and ANOVA (a generalization of the t -test and is suited to more complex comparisons than the t -test) to be considered as options for comparing mean and spread of data [18]–[20]. However, the results for the t -test of both comparisons indicate

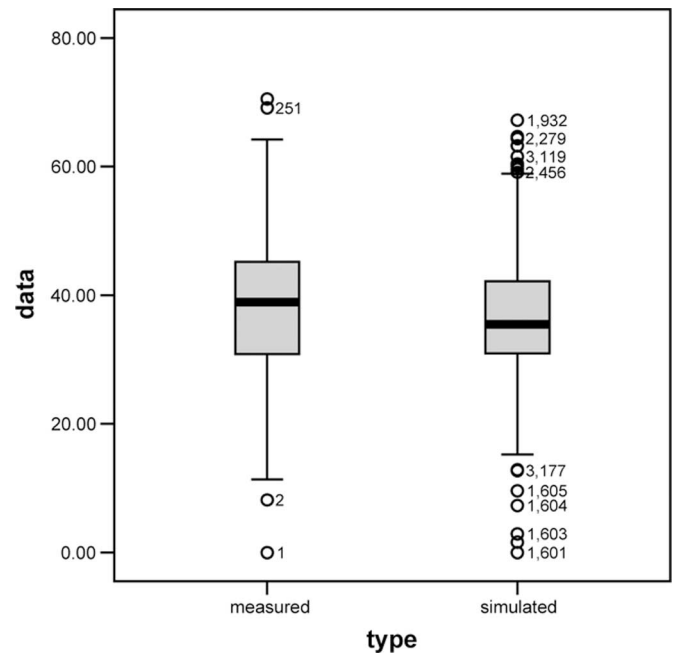


Fig. 19. Box plot of the current ratio data of Fig. 10.

that there is a significant difference in the mean values for the two groups.

These tests give an indication of the level of overall agreement between the data sets being compared and suggests that there is a poor agreement on a point-by-point basis, or when considering the level of agreement of the mean values. However, the shape of the probability distributions has not been considered. Non-parametric tests, so called because they make no assumptions of distribution normality, but do take the shape of the probability distributions into account. The most popular techniques

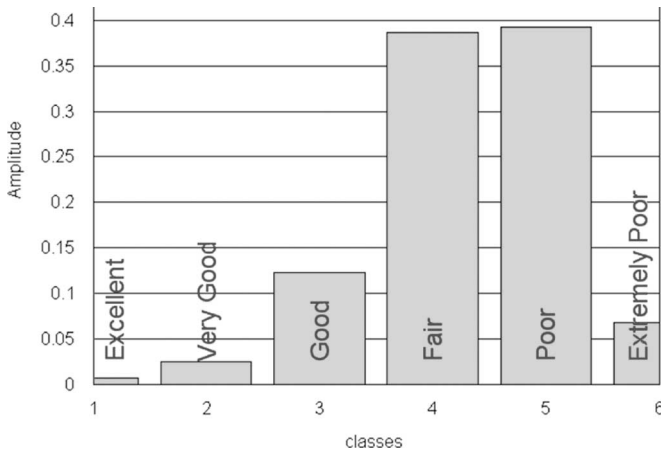


Fig. 20. GDM confidence histogram for the stirring ratio data of Fig. 4.

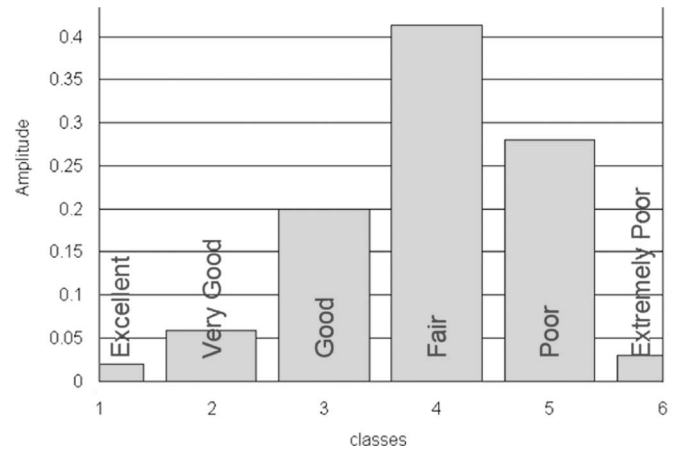


Fig. 21. GDM confidence histogram for the current ratio data of Fig. 10.

in electromagnetics, and particularly, reverberation chamber assessment, are the χ^2 test and the KS test [22] ([22] also provides a good introduction to these tests, and further information can be found in [18] and [23]). The χ^2 test measures a level of association (causal relationship) between the two results, and when applied to the data, suggests that there is a significant difference between the pairs. However, it is inappropriate because it is clear from the analysis so far that there is a notable difference between the results, but the χ^2 test does not help to provide a more meaningful interpretation of this difference. The KS test makes an assessment of whether there is sufficient evidence to reject the null hypothesis that the two data sets are the same. The results of applying the KS test to the data of Figs. 4 and 10 suggest that the distributions of the simulated and measured results are significantly different. Unfortunately, as noted with the box-plot results, there are many outliers that may have bearing on the distributions.

The final approach considered in this paper was developed to provide an algorithmic quantification in the manner that experienced engineers would do by eye. This is the FSV method [24]. The FSV works by decomposing the original data to be compared into the envelope and rapidly changing feature data sets. Comparison of these provides an amplitude difference measure (ADM) and a feature difference measure (FDM), which can be combined into an overall goodness-of-fit: global difference measure (GDM). Hence, the FSV provides an assessment of the two data sets to be compared based more on how the graphs align rather than on the probability of values. A particular feature that is helpful in order to aid interpretation is the fact that the output data can be partitioned into a number of natural language equivalent categories, as in Fig. 13, and a resulting histogram produces a measure of confidence in a summary value. This confidence histogram provides a close analogy of the response of a large group of experts visually inspecting the data [22]. Applying the FSV method to the data in Figs. 4 and 10 results in the GDM confidence histograms [26], [27] of Figs. 20 and 21.

These figures show that the comparison of the current on the wire is overall better than the stirring ratio comparison, both

of these agreeing well with the visual interpretation of Figs. 14 and 15.

V. DISCUSSION AND CONCLUSION

The purpose of this paper was to assess whether a coarse implementation of a TLM model of a reverberation chamber provided a sufficiently high level of agreement to merit “validation.”

Results looking at stirring ratio and also comparing simulated and experimental currents on a wire were presented both graphically and numerically. The graphical results showed many similarities between the models and measurements, and the numerical results were accurate to within a few decibels.

In an attempt to quantify the levels of agreement, two representative worst case data sets were compared visually by a number of reverberation chamber knowledgeable engineers. Further, statistical and heuristic techniques were applied in an attempt to quantify the results. Statistical tests suggested that there was insufficient evidence to accept that the pairs of results compared had a high probability of coming from the same populations. The FSV method suggested that the level of agreement is not high, but there is a reasonable level of agreement: an assessment that agrees quite closely with the visual assessment.

One potential problem with applying statistical tests to this data is that they are based on some comparison of mean levels and/or probability distributions and the mean levels and distributions may change along the independent axis. In this case, it was noted that the stirrer becomes electrically large above approximately 300 MHz, and hence, it may be assumed that there could be different responses above and below this level. Fig. 4 shows that this may be the case where, below 300 MHz, there is a clear difference in the apparent mean values, but above this, the mean levels appear to be much closer. Similarly, all the results presented have a very high feature density. While no quality judgment is made as to whether the “grassiness” is noise or closely spaced high- Q features, the noncollocation of features does have a substantial impact on distribution-based statistics.

The question remains: can it be claimed that a TLM model of a reverberation chamber that is modeled with a coarse mesh,

a limited iteration count, and undersampled stirrer positioning provides an acceptable model of the actual system? The limitations of the models being considered can be seen from the comparison of run times against the theoretical system, where the fields had been allowed to decay much more than in this case. The stirrer height tests were completed over a weekend; however, to run for 600 000 iterations would have taken several years. The evidence suggests that the comparison is satisfactory, which, considering the coarseness of the model, is in fact, very favorable. Considering that the stated goal was not to seek perfection on simulation quality but to “satisfice,” this goal has been reached.

The techniques used in this research could be useful in supporting additional studies that have emerged from this paper, such as:

- 1) addressing the level of impact each of the key assumptions have on the overall comparisons;
- 2) quantifying the quality of simulations produced by several modelling techniques.

Both of these would be valuable contributions to the study of reverberation chambers.

ACKNOWLEDGMENT

The authors would like to acknowledge the invaluable assistance of Messrs. S. Gillett, T. O’Mara (De Montfort University), C. Ritota, and F. Campitelli (University of L’Aquila).

REFERENCES

- [1] A. Drozd, “Progress in development of standards and recommended practices for CEM computer code modeling and code validation,” in *Proc. 2003 IEEE Int. Symp. EMC*, vol. 1, pp. 313–316.
- [2] W. C. Stirling, *Satisficing Games, and Decision Making: With Applications in Engineering and Computer Science*. Cambridge, U.K.: Cambridge Univ. Press, 2003.
- [3] P. Corona, J. Ladbury, and G. Latmire, “Reverberation chamber research—Then and now: A review of early work and comparison with current understanding,” *IEEE Trans. Electromagn. Compat.*, vol. 44, no. 1, pp. 87–94, Feb. 2002.
- [4] K. Madsen, P. Hallbjørner, and C. Orlenius, “Models for the number of independent samples in reverberation chamber measurements with mechanical, frequency, and combined stirring,” *IEEE Antennas Wireless Propag. Lett.*, vol. 3, no. 1, pp. 48–51, 2004.
- [5] H.-J. Asander, G. Eriksson, L. Jansson, and H. Akermark, “Field uniformity analysis of a mode stirred reverberation chamber using high resolution computational modelling,” in *Proc. IEEE Int. Symp. EMC*, 2002, pp. 285–290.
- [6] D. I. Wu and D. C. Chang, “The effect of an electrically large stirrer in a mode-stirred chamber,” *IEEE Trans. Electromagn. Compat.*, vol. 31, no. 2, pp. 164–169, May 1989.
- [7] P. Bonnet, R. Vernet, S. Girard, and F. Paladian, “FDTD modelling of reverberation chamber,” *Electron. Lett.*, vol. 41, no. 20, pp. 1101–1102, Sep. 2005.
- [8] M. R. Zunoubi, C. D. Taylor, A. A. Kishk, and H. A. Kalhor, “Electromagnetic modelling of 2D electronic mode stirred reverberating chambers for electromagnetic compatibility and interference analysis and design,” *J. RF Microw. Comput.-Aided Eng.*, vol. 15, no. 2, pp. 197–202, Mar. 2005.
- [9] A. R. Coates, A. P. Duffy, K. G. Hodge, and A. J. Willis, “Validation of mode stirred reverberation chamber modelling,” in *Proc. Int. Symp. EMC*, Sorrento, Italy, 2002, pp. 35–40.
- [10] C. Bruns and R. Vahldeick, “A closer look at reverberation chambers—3D simulations and experimental verification,” *IEEE Trans. Electromagn. Compat.*, vol. 47, no. 3, pp. 612–626, Aug. 2005.
- [11] P. Hallbjørner, “A model for the number of independent samples in reverberation chambers,” *Microw. Opt. Technol. Lett.*, vol. 33, no. 1, pp. 25–28, Apr. 2002.
- [12] C. L. Holloway, D. A. Hill, J. M. Ladbury, and G. Koepke, “Requirements for an effective reverberation chamber: Unloaded or loaded,” *IEEE Trans. Electromagn. Compat.*, vol. 48, no. 1, pp. 187–194, Feb. 2006.
- [13] W. Joseph and L. Martens, “The influence of the measurement probe on the evaluation of electromagnetic fields,” *IEEE Trans. Electromagn. Compat.*, vol. 45, no. 2, pp. 339–349, May 2003.
- [14] B.-H. Liu, D. C. Chang, and M. T. Ma, “Eigenmodes and the composite quality factor of a reverberating chamber,” *Natl. Bur. Stand., Gaithersburg, MD, Tech. Note TN-1066*, 1983.
- [15] C. Christopoulos, *The Transmission Line Modeling Method in Electromagnetics* (Synthesis Lectures on Computational Electromagnetics), 2006, Morgan and Claypool Publishers.
- [16] F. Moglie, “Convergence of the reverberation chambers to the equilibrium analyzed with the finite-difference time-domain algorithm,” *IEEE Trans. Electromagn. Compat.*, vol. 46, no. 3, pp. 469–76, 2004.
- [17] D. E. Coleby and A. P. Duffy, “A visual interpretation rating scale for the validation of numerical models,” *COMPEL*, vol. 24, no. 4, pp. 1078–1092, 2005.
- [18] StatSoft, Inc., 2006, *Electronic Statistics Textbook*. Tulsa, OK: StatSoft, 2006. [Online]. Available: <http://www.statsoft.com/textbook/stathome.html>.
- [19] D. G. Rees, *Essential Statistics*, 4th ed. Boca Raton, FL: Chapman & Hall/CRC Press, 2000.
- [20] J. Devore and R. Peck, *Statistics: The Exploration and Analysis of Data*, 2nd ed. Belmont, CA: Duxbury, 1993.
- [21] T. T. Soong, *Fundamentals of Probability and Statistics for Engineers*. West Sussex, U.K.: Wiley, 2004.
- [22] P. Corona, G. Ferrara, and M. Migliaccio, “Reverberating chambers as sources of stochastic electromagnetic fields,” *IEEE Trans. Electromagn. Compat.*, vol. 38, no. 3, pp. 348–356, Aug. 1996.
- [23] W. J. Conover, *Practical Nonparametric Statistics*. New York: Wiley, 1980.
- [24] A. P. Duffy, A. J. M. Martin, A. Orlandi, G. Antonini, T. M. Benson, and M. S. Woolfson, “Feature selective validation (FSV) for validation of computational electromagnetics (CEM). Part I—The FSV method,” submitted for publication.
- [25] A. Orlandi, A. Duffy, B. Archambeault, G. Antonini, D. Coleby, and S. Connor, “Feature selective validation (FSV) for validation of computational electromagnetics (CEM). Part II—Assessment of FSV performance,” submitted for publication.
- [26] A. Orlandi. (2007). Free stand-alone FSV application, [Online]. Available: <http://ing.univaq.it/uaqemc/public.html/>.
- [27] A. Duffy. (2006). Feature selective validation, [Online]. Available: <http://www.eng.cse.dmu.ac.uk/FSVweb/>.



Alyse Coates received the M.Eng. degree in electrical and electronic engineering from the University of Nottingham, Nottingham, U.K., in 1997, and the Ph.D. degree from De Montfort University, Leicester, U.K., in 2004.

She was the Experimental Officer with the George Green Institute for Electromagnetics Research, Nottingham University, where she was responsible for the high-frequency measurement facility.

She joined the Applied Electromagnetics Group, De Montfort University, Leicester, U.K., in 1999.



Hugh G. Sasse received the B.Sc.(Hons.) degree in electronic engineering from the University of York, York, U.K., in 1985, and is currently working toward the Ph.D. degree in optimization of physical layer components for communications systems at De Montfort University, Leicester, U.K.

His current research interests include computer modeling of novel antenna structures and other communication channel components with an emphasis on optimization of such structures.



Dawn E. Coleby received the Honours degree in medical and health statistics from De Montfort University, Leicester, U.K., in 2000, and the Ph.D. degree from De Montfort University, Leicester, U.K., in 2004.

She is currently a Research Associate in the Department of Health Sciences, University of Leicester, Leicester.



Alistair P. Duffy (M'93–SM'04) was born in Ripon, U.K., in 1966. He received the B.Eng. degree in electrical and electronic engineering from University College, Cardiff, U.K., in 1988, the M.Eng. degree from University College, Cardiff, U.K., in 1989, the Ph.D. degree from Nottingham University, Nottingham, U.K., in 1993, and the MBA degree from the Open University, in 2004.

He is currently a Reader in Electromagnetics and the Head of the Engineering Division, De Montfort University, Leicester, U.K. His current research interests include CEM validation, communications cabling, and technology management. He is the author or coauthor of over 100 papers published in journals and international symposia.

Dr. Duffy is a Fellow of the Institution of Engineering and Technology (IET) and a member of the Chartered Management Institute, the International Com-pumag Society, and the Applied Computational Electromagnetics Society.



Antonio Orlandi (M'90–SM'97–F'07) was born in Milan, Italy in 1963. He received the Laurea degree in electrical engineering from the University of Rome "La Sapienza," Rome, Italy, in 1988.

From 1988 to 1990, he was with the Department of Electrical Engineering, University of Rome "La Sapienza." Since 1990, he has been with the Department of Electrical Engineering, University of L'Aquila, L'Aquila, Italy, where he is currently a Full Professor at the UAq EMC Laboratory. He is the author or coauthor of more than 100 published technical

papers in the field of electromagnetic compatibility in lightning protection systems and power drive systems. His current research interests include numerical methods and modeling techniques to approach signal/power integrity, electromagnetic compatibility/electromagnetic interference issues in high-speed digital systems.

Dr. Orlandi received the IEEE Transactions on Electromagnetic Compatibility Best Paper Award in 1997, the IEEE Electromagnetic Society Technical Achievement Award in 2003, the IBM Shared University Research Award in 2004 and 2005, and the CST University Award in 2004. He is a member of the Education, TC-9 Computational Electromagnetics and the TC-10 Signal Integrity Committees of the IEEE EMC Society, and the Chairman of the "EMC INNOVATION" Technical Committee of the International Zurich Symposium and the Technical Exhibition on EMC. From 1996 to 2000, he was an Associate Editor of the IEEE TRANSACTIONS ON ELECTROMAGNETIC COMPATIBILITY and currently serves as Associate Editor of the IEEE TRANSACTIONS ON MOBILE COMPUTING.